Contents lists available at ScienceDirect

Arabian Journal of Chemistry

journal homepage: www.ksu.edu.sa

Sustainable biosorption of Methylthioninium Chloride in wastewaters using new *Cystoseira barbata* seaweed: Equilibrium isotherm, kinetic modeling and mechanism analysis

Hafssa Atlas [a], Mohamed Sadoq [a], Smail Imame [a], Abdelouahed Amar [a], Abderahim Kali [a], Ilyasse Loulidi [a], F.Z. Mamouni [a], Maria Jabri [a], Hadey Chaimaa [a], Mohammed Naciri Bennani [a], A. Palsan Sannasi [b], Fatima Boukhlifi [a,*]

[a] *Laboratory of Chemistry and Biology Applied to the Environment, URL-CNRST-N◦13, Faculty of Sciences, Moulay Ismail University, Meknes 50050, Morocco*
[b] *Faculty of Agro-Based Industry, Universiti Malaysia, Kelantan Jeli Campus, Jeli, Kelantan 17600, Malaysia*

ARTICLE INFO

Keywords:
C.*barbata*
Methylthioninium Chloride
Seaweed
Morocco
Dye
Adsorption

ABSTRACT

Due to its climatic diversity and geographical position, Morocco is one of the most productive countries of seaweed in the world. This work aims to study the Methylthioninium Chloride (referred to as Methylene Blue) adsorption from wastewater using raw marine seaweed C.*barbata* that are considered as one of the important algae that are responsible for pollution in the Mediterranean Sea. different factors such as biomass dose, pH, and contact time were examined to demonstrate their impact on the biosorption process. The contact time studied revealed that biosorption of Methylene Blue reached equilibrium in 55 min. The biosorption data was subjected to the kinetic models Pseudo-first and pseudo-second order. Pseudo second order model was aligned with the adsorption data, whereas data didn't fit pseudo first order model. Adsorption data were modelled with Freundlich and Langmuir isotherm equations at room temperature. The maximum adsorption capacity estimated was 29.56 mg/g based on Langmuir isotherm model. Thus, C. *barbata* can be regarded as a valuable natural biosorbent for the treatment of wastewaters containing toxic dyes.

1. Introduction

Water pollution generated by organic and inorganic chemicals is a major dilemma producing environmental degradation (Amar et al., 2021). Synthetic dyes are one of the most remarkable problems widely caused by the rapid urbanization and industrial development, which can cause a severe damage to the aquatic environment and living organisms present in water (Gupta et al., 2003). Dyes and pigments are used in pharmaceutical industries, dying of leather, paper, plastic, and cosmetic products. They are resistant to light and heat, and immune to aerobic digestion, (Jayganesh et al., 2017) Due to their chemical stability, dyes are difficult to be removed from wastewaters (Nassar and Magdy, 1997). Currently, researchers have investigated several treatment processes, namely ultrafiltration (Saffaj, 2004), chemical oxidation (Usman, 2018), photocatalytic degradation (Abbood et al., 2023; Naciri et al., 2018) and bioremediation (Jabbar et al., 2022), to reduce the toxicity of synthetic dyes or get rid of them. However, these methods can be extremely expensive, and suffer from limitations due to the complexities in the regeneration of the substrate (Sen et al., 2011) and most of them are not able to remove dyes entirely from wastewater (Kumar et al., 2015). Consequently, researchers have been focused on improving and identifying an alternative technique to remove toxic substances from water. Adsorption has gained interest and became the most used technique in industrial applications (Khatri et al., 2018), because of its ease of operation, low initial cost and ecofriendly nature sorption with biomaterials. Biosorption is used for the removal of heavy metals and dyes (Loulidi, et al., 2019; Boukhlifi et al., 2001), aromatic substances (Ali et al., 2023), sulfur compounds (Al-Khodor and Albayati, 2023; Khadim et al., 2022); organic carbon (TOC) and turbidity (Ali et al., 2022), and contaminations from aqueous solutions. According to many studies, raw seaweed showed high efficiency in removing toxic pollutants from aqueous solutions, (Ainane, 2014; Belattmania, 2015; Chu and Hashim, 2007) they were also used after chemical modifications (Ainane, 2014; Essekri, 2020)Seaweed derived alginate (Belattmania

* Corresponding author.
E-mail address: f.boukhlifi@umi.ac.ma (F. Boukhlifi).

https://doi.org/10.1016/j.arabjc.2023.105532
Received 26 July 2023; Accepted 4 December 2023
Available online 5 December 2023

et al., 2017), polysaccharide, biochars (Katiyar et al., 2021), Carrageenan (Sharma et al., 2022), activated carbon (Jayganesh et al., 2017) have been proven to be an excellent adsorbent for wastewater treatment. Marine algae have shown the ability to remove dyes from wastewaters due to its high affinity because of the richness of its functional groups, namely as, amino, carboxyl, sulfate and hydroxyl, (Lesmana et al., 2009) that act as biding sites for the biosorption. Indeed, several species are used as biosorbents of dyes from aqueous solutions, particularly, *Cystoseira barbata*, this brown seaweed is abundantly available in the Mediterranean Sea, and known for its negative ecological impact. Yet, it can be employed as a promising biosource for the adsorption of wastewater decontamination. There are several studies on seaweed used as biosorbents to treat different dyes in order to discover their adsorption capacities. For instance, brown alga *Cystoseira barbatula Kützing* that was used for the adsorption of Methylene Blue (Caparkaya and Cavas, 2008). The maximum capacity found in the study is 38.61 mg/g at 35 °C. for the treatment of the same pollutant, *Caulerpa racemosa* var. *cylindracea* (Cengiz and Cavas, 2008), *Sargassum muticum* (El Atouani et al., 2019) *and Posidonia oceanica* (Ncibi et al., 2007) were used, and the maximal capacity obtained was 5.23 mg/g at 18 °C, 191.38 mg/g at 25 °C and 5.56 mg/g at 30 °C respectively. Methylene blue For instance, is an organic dye largely used by industries to dye materials, and it was employed in clinical settings for the identification of pathologic structures (Cragan, 1999). Methylene Blue can also cause serious health problems when it is used recklessly, (Chcn et al., 1999) it can also cause eye burns and injury (Kali, 2022). In this respect, it is important to improve Methylene Blue dye removal methods. The aim of this paper is to characterize the performance of *Cystoseira barbata* brown seaweed on the biosorption of methylene blue contained in aqueous solutions. The optimization of the treatment process and the study of the effect of some parameters such as pH, mass, temperature on adsorption of the dye on the algae was undertaken. The analysis of the retention mechanism and explanation of the surface interactions between the pollutant and algae were studied by the physicochemical characterization of the adsorbent before and after adsorption.

2. Materials and methods

2.1. Adsorbate

Methylthioninium Chloride (MB) is the dye used in this study, its chemical structure is shown in Fig. 1. MB was used without additional purification. Different concentrations were prepared using distilled water. Initial concentrations of Methylene blue solutions were attained by measuring the adsorption at a wavelength λ_{max} 670 nm using UV/Visible spectrophotometry.

2.2. Adsorbent

Cystoseira barbata was collected from Nador lagoon in the Moroccan Mediterranean coastline. The seaweed was swept many times with tap water and distilled water thereafter to illuminate salts and external waste. subsequently, it was dehydrated in room temperature for 72 h and grounded to obtain a powder.

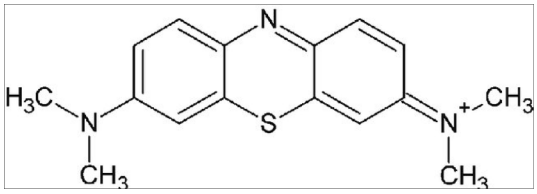

Fig. 1. Methylene blue structure.

2.3. Characterization of the seaweed

Various instrumental techniques were employed to examine the solid surface, derived from several experiments and preparations conducted in this study, specifically FTIR and SEM alongside an energy dispersive analysis system (EDS).

The samples were prepared by combining 95 mg of KBr with 5 mg of the seaweed powder. The resulting combination (seaweed/KBr) was ground thinly using an agate mortar, and compressed subsequently under the weight of 4 tons using a pelletizer to produce thin pellets, that were positioned in the IR beam path. Schimadzu JASCO 4100 instrument revealed only adsorption bands recorded by the solid utilized, due to the transparency of potassium chloride within the scope of 4000 cm^{-1} to 400 cm^{-1}. The resolution of all spectrums recorded is 4 cm^{-1} and 64 scans.

2.4. Biosorption experiments

All experiments were performed at room temperature (25 ± 2 °C), a known amount of the studied seaweed was put into 40 ml flacon tube and treated with 20 ml of the dye solution. Experiments were obtained by varying adsorbent dosage (50–300 mg/L), contact time (5–120 min), initial pH (2–12) that was adjusted to the value required using 1 M HCl or 1 M NaOH solution, and initial concentration of methylene blue (5–400 mg/L). The final concentration of the dye was determined by measuring the absorbance utilizing a spectrophotometer UV/Visible at a wavelength of λ_{max} 670 nm. The amount in ($mg.g^{-1}$) of MB adsorbed (Qe) into the seaweed as well as the removal efficiency R (%) was calculated respectively from Eqs. (1) and (2).

$$Qe = \frac{(C0 - Ce)*V}{m} *100 \quad (1)$$

$$R(\%) = \frac{C0 - Ce}{C0} *100 \quad (2)$$

Where C_0 is the initial concentration, V(L) is the initial volume of dye solution and C_e ($mg.L^{-1}$)is the concentration of methylene blue solution at equilibrium.

3. Results and discussion

3.1. 3.1.Characterization of the adsorbent

3.1.1. Point of zero charge

The point of zero charge (pH_{PZC}) curve is presented in Fig. 2.

The point of zero charge (pH_{PZC}) is an essential factor that provides information about the surface charge of biosorbents. At this pH, the

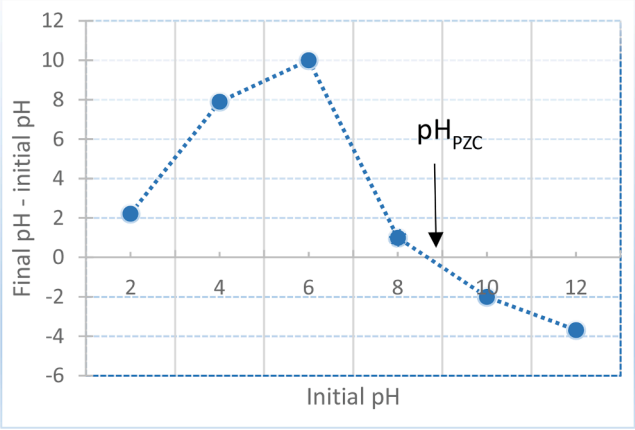

Fig. 2. Point of zero charge of *C. barbata*. biomass.

surface presents a neutral charge due to the equal amount of positive and negative surface sites, which characterizes the ionization of functional groups in the adsorbent and their interactions with dye species in solution. According to Fig. 2, pH_{pzc} value is equal to 8.6 ± 0.1, therefore, the seaweed surface is negatively charged above this value and positively charged bellow it.

3.1.2. Analyse by FTIR

Fig. 3 shows the IR spectrum relating to the adsorbent material.

C. barbata. was examined using Fourier Transform Infrared Spectrometry analysis (FTIR) to determine the functional groups on the biomass surface. Fig. 3 shows the main peaks that were detected. The main functional groups of raw seaweed are listed bellow:

- The large band at 3404 cm^{-1} corresponds to the O—H and N—H groups.
- The peak at 2931 cm^{-1} is attributed to the symmetrical stretching vibration of C—H bonds in aliphatic chains.
- The band at 1662 cm^{-1} corresponds to amide II.
- The peak at 1436 is attributed to the —CH_2—and—CH_3.
- the peak at 1033 cm^{-1} corresponds to S═O group.

3.1.3. Analyse the surface by SEM

Scanning electron microscopy (SEM) is an essential tool to observe the morphology of *C. barbata* (Ali et al., 2022). Figs. 4 and 5 present SEM image and EDS spectrum of C. *barbata*.

Fig. 4 indicates the presence of micro pores on the surface of the sample favorable for an efficient diffusion of the dye molecules.

The EDS spectrum of *C.barbata* confirms the existence of oxygen and carbon as major constituents of the material.

The surface is very porous compared to other surfaces of marine origin such as chitin (Boukhlifi and Bencheikh, 2000) and agricultural origin such as coconut, almond, walnut, peanut shells and spent coffee grounds (Kali et al., 2022; Jabri et al., 2023; Amar et al., 2021; Kali et al., 2022; Loulidi et al., 2020; Loulidi et al., 2020) The pores are very distinct and can trap polluting molecules. In addition to this porous surface, the presence of oxygen in the structure of the molecules offers very negative sites capable of attracting positive surfaces.

3.2. Analysis of adsorption optimum conditions

3.2.1. Effect of initial pH

Fig. 6 presents the impact of pH on the biosorption process.

The pH of the solution is considered significant in this process since it has an effect on the protonation of the functional groups of seaweed in addition to the ionization of the dye in aqueous solutions. The influence of pH was evaluated by agitating 3 mg of biosorbent for 2 h in 20 ml of MB solution at room temperature (25 °C). The biosorption was examined within a pH ranging from 2 to 12. pH was adjusted using NaOH 1 M or HCl 1 M solutions. Highest optimum uptake value that was found at pH 8 is probably due to the electrostatic attraction between the surface

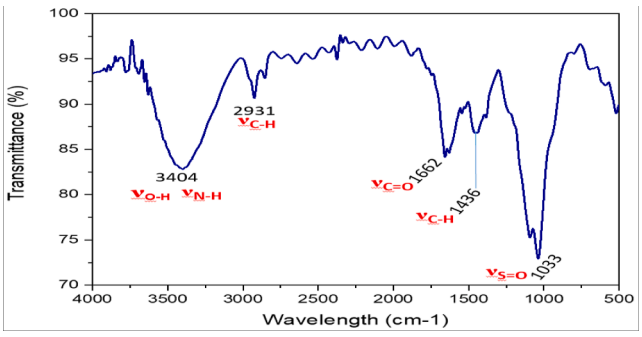

Fig. 3. FTIR spectrum of *C.barbata*.

of seaweed biomass that is negatively charged and the cationic dye MB. Low values of the quantity adsorbed at acid pH can be explained by the excess of protons in the solution competing with MB cations for spots on the seaweed surface area, therefore, decreasing the amount of methylene blue adsorbed in acidic conditions.

3.2.2. Effect of biosorbent mass

Biosorption process is examined by the dose of the adsorbent. Fig. 7 shows the influence of *C. barbata* dosage for MB adsorption.

Due to the availability of sites on the seaweed area, efficiency of the biosorption increases with adsorbent mass. The biosorbent dose was evaluated by varying the amount of *C. barbata* from 1 mg to 6 mg at room temperature, and then added to individual 20 ml samples of an aqueous solution containing 5.10^{-5} M of the dye for 1 h. According to the figure, the removal percentage of the dye reached the peak at 3 mg per 20 ml of MB solution. After this dosage, which is considered to be optimum, the adsorption percentage remained almost constant.

3.2.3. Effect of the contact time

Fast adsorption equilibrium is an important factor influencing the biosorption efficiency. The impact of time on the biosorption process is presented in Fig. 8.

The equilibrium time needed to adsorbe methylene blue dye by *C. barbata* was determined by adding 3 mg of the dried biomass in 20 ml of a solution containing 5.10^{-5} M of the dye solution at a temperature of 25 ± 2 °C. Time was varied from 5 to 120 min. Results in Fig. 8 show a fast removal of MB in the first 20 min, Due to the availability of reactive groups of the adsorbent surface in the beginning. Thereafter, the equilibrium was reached after 55 min of contact time.

3.3. Isotherm study

3.3.1. Kinetic study

Understanding the mechanism of adsorption is a key role in the dye removal process. Adsorption kinetics were modeled using the pseudo-first order and pseudo-second order models.

The linear form of pseudo first order model is:

$$\mathrm{Log}(q_e - \mathrm{q}) = \mathrm{Loq}(q_e) - \frac{K_1 \mathrm{t}}{2.303}$$

Where:

Qe (mg/g) is the adsorption capacity or the amount of adsorbate adsorbed at equilibrium, **q** (mg/g) is the adsorption capacity at a given time t, $\mathbf{K_1}(min^{-1})$ is the rate constant of pseudo first order, and **t** is the contact time (min).

The linear form of pseudo second order model is:

$$\frac{t}{q_t} = \frac{1}{K_2 * q_e^2} + \frac{t}{q_e}$$

Where:

$\mathbf{K_2}$ ($g.mg^{-1}.min^{-1}$) is the constant rate of pseudo second order.

The parameter values of pseudo-first order and pseudo-second order rate constants (K_1) and (K_2) successively, equilibrium adsorption capacity (q_e) and the corresponding regression coefficient (r^2) were calculated and listed in Table 1. Fig. 9 presents First-order sorption kinetic and Fig. 10 presents second-order adsorption kinetics of MB by seaweed.

The suitable model established for this study is chosen based on the correlation factor. The higher this coefficient, the more the model is fitted for the study of the adsorption of MB. The obtained results in Table 1 show that pseudo-first order correlation factor (r^2 = 0.49) is lower than that of the pseudo-second order (r^2 = 0.99). On the other hand, the absence of linearity at the plot line of $\ln(C_0\text{-}C_t)$ versus t (Fig. 9) shows that the adsorption process of MB did not follow the pseudo-first order kinetic model. Accordingly, the kinetic model providing the best fit to the biosorption experiment is the pseudo-second order (Fig. 10)

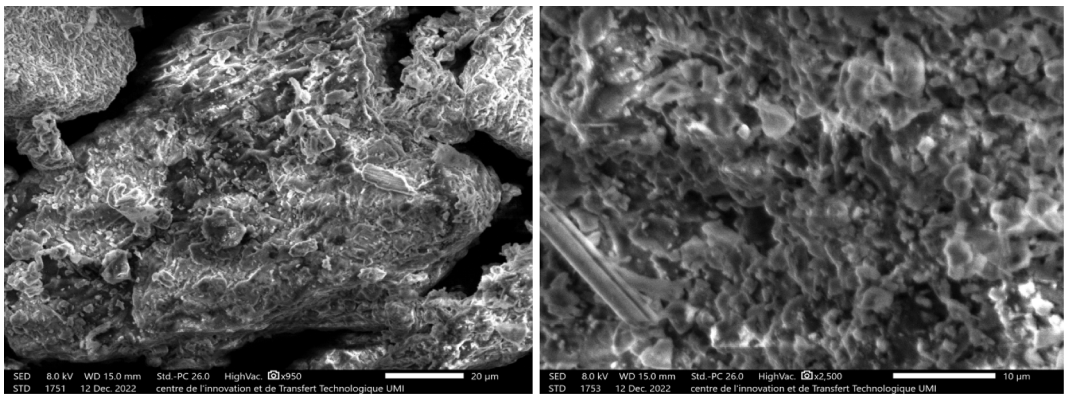

Fig. 4. SEM images of *C.barbata.*

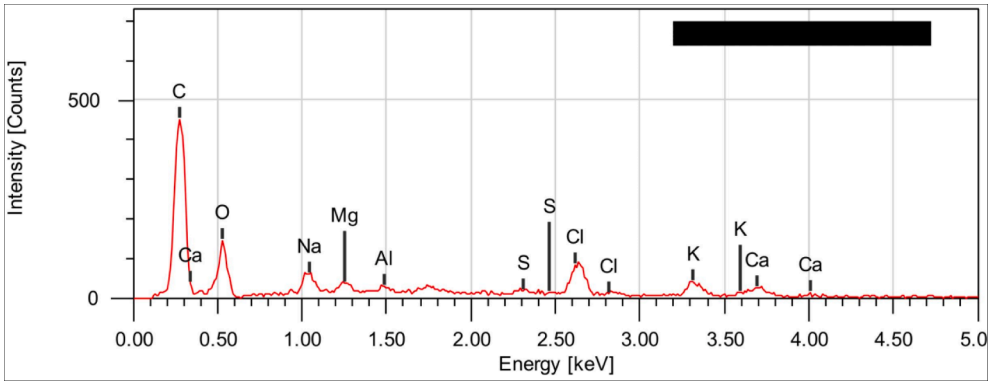

Fig. 5. EDS spectrum of *C. barbata.*

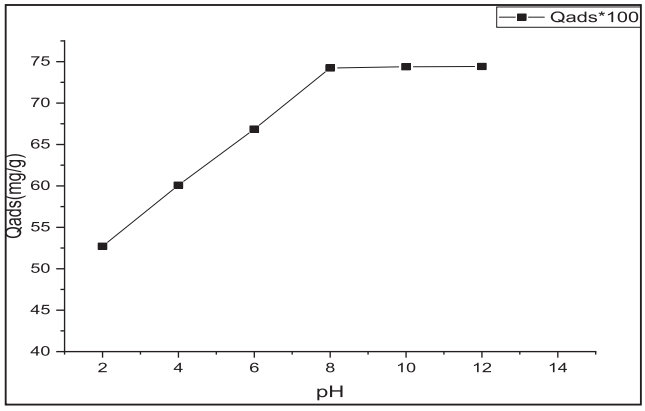

Fig. 6. Effect of pH on the biosorption process.

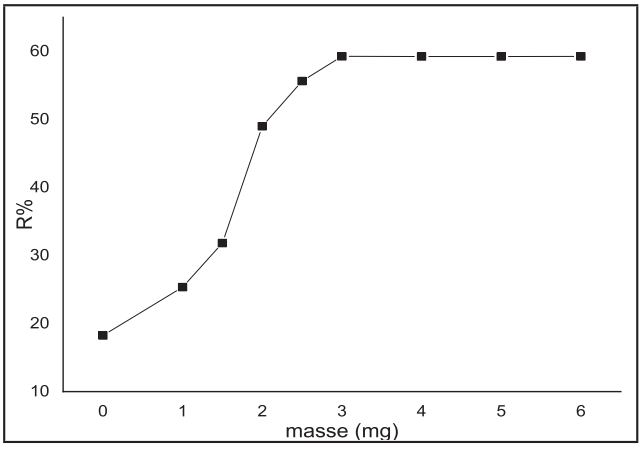

Fig. 7. Effect of adsorbent dose on efficiency of the biosorption.

which describes better the adsorption process of MB on *C. barbata* surface. This model suggests that the biosorption was controlled by chemisorption, (Zhang et al., 2013) which involves interactions between the adsorbent and functional groups of the adsorbate surface.

3.3.2. *Isotherm study: Modeling of adsorption isotherms*

Adsorption isotherm describes the variation of the quantity adsorbed by the material and the total amount of adsorbate in the solution at a consistent temperature. It is useful to optimize the experimental conditions in order to obtain maximum dye uptake. It is explained by models that provide important information about the distribution of the adsorbate on material surface based on assumptions about the homogeneity or heterogeneity of the surface and interactions probable between the adsorbate and type of coverage (Heo et al., 2018). Freundlich and Langmuir isotherms were used for the biosorption of MB by *C. barbata.* Langmuir model predicts the monolayer of MB on the adsorbent surface, and its expression (Yemendzhiev et al., 2021) can be written as:

$$\frac{C_e}{q_e} = \frac{1}{q_{max} K_L} + \frac{C_e}{q_{max}}$$

Where q_e ($mg.g^{-1}$) is the equilibrium adsorbed quantity of methylene blue, K_L is the Langmuir constant, C_e ($mg.L^{-1}$) is the concentration of methylene blue at equilibrium, and q_{max} (mg/g) is the maximum adsorption capacity. On the other hand, Freundlich model is applied to

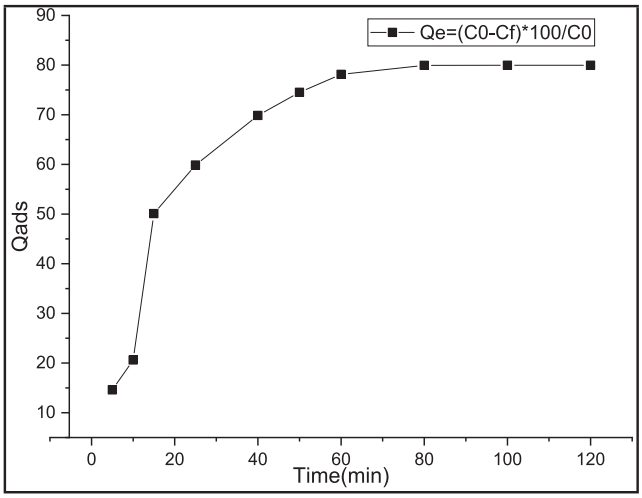

Fig. 8. Effect of time.

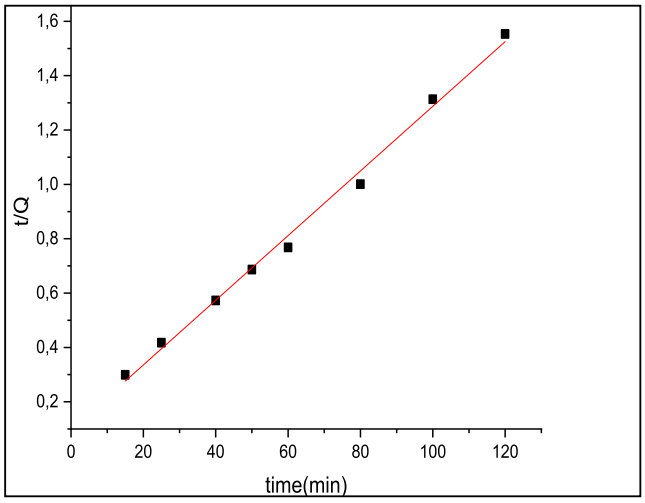

Fig. 10. Second-order adsorption kinetics of MB by seaweed.

Table 1
Pseudo first and second order adsorption kinetics for adsorption of MB onto seaweed.

pseudo-first order kinetic model	r^2	Q_e (mg.g^{-1})
	0.499	21.159
pseudo-second order kinetic model	r^2	Q_e (mg.g^{-1})
	0.99	21.59

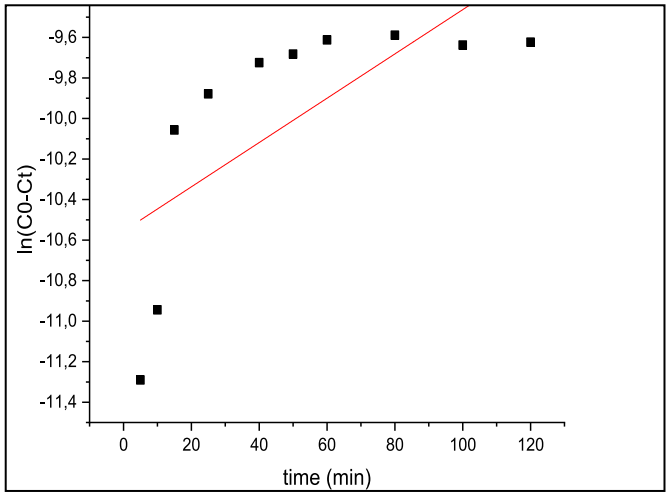

Fig. 9. First-order sorption kinetic of MB by seaweed.

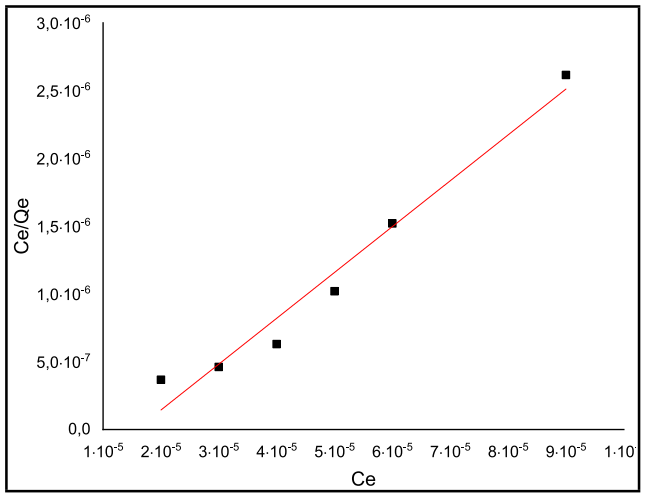

Fig. 11. Langmuir isotherm for MB.

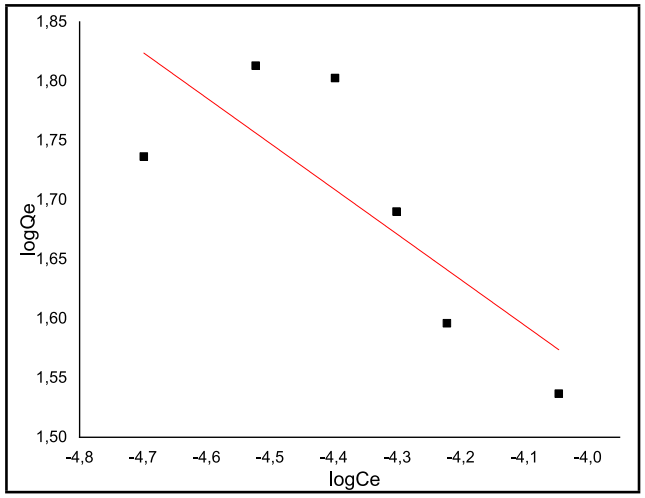

Fig. 12. Freundlich isotherm for MB.

the heterogeneous surfaces and predicts the multi-layer biosorption of the dye on the material surface. and its expression (Maaloul et al., 2017) is given bellow:

$$\log q_e = logK_f + \frac{1}{n} logC_e$$

Where K_f is the Freundlich constant and n is a parameter that varies with degree of heterogeneity of the adsorbent surface. Fig. 11 presents Langmuir isotherm and Fig. 12: presents Freundlich isotherm for MB. Table 2 presents Freundlich and Langmuir models for the biosorption of methylene blue by C. barbata.

The reliability of Langmuir and Freundlich isotherms was evaluated by calculating the correlation coefficients R^2. As can be seen from Table 2, regression coefficient obtained by Langmuir model is higher ($R^2 = 0.96$) than that of Freundlich model ($R^2 = 0.62$). The applicability

Table 2
Freundlich and Langmuir models for the biosorption of methylene blue by C. barbata.

Langmuir model			Freundlich model		
Q_{max}	K_L	R^2	K_F	1/n	R^2
29.55956	0.00635	0.96	−0.028	−2.61	0.62

of Langmuir isotherm model inferred that the adsorption of MB onto C. *barbata* is assumed as a monolayer adsorption. The plot of log q_e versus log C_e describes Freundlich isotherm for the adsorption of MB by C. *barbata*. Freundlich constants are shown in Table 2. It is important to identify The q_{max} value that is the maximum value of the quantity adsorbed at equilibrium, the value of q_{max} found was 29.56 mg/g.

Table 3 presents the maximum adsorption capacities of different seaweed. compared to the other adsorbents, c.*barbata* can be considered an alternative source for MB removal from aqueous solutions.

3.3.3. Thermodynamic study

Fig. 13 represents the thermodynamic study of the energetic changes in the adsorption of Methylene blue by raw seaweed. And thermodynamic parameters are listed in Table 3.

The effect of temperature was evaluated by agitating 3 mg of biosorbent for 2 h in 20 ml of MB solution. Then placed in flasks with different temperatures (25, 30, 35, 40, 45 °C) in a thermostatic water bath.

Many studies have proved that adsorption process is highly affected by the temperature. According to adsorption theory, increasing the temperature generates a decrease in ad0sorption reaction due to the desorption, at high temperatures, of molecules adsorbed earlier from the surface. To determine the optimum temperature value, different temperatures were investigated varying from 25 °C to 45 °C. 3 mg of biosorbent was placed in 20 ml of MB solution for 2 h in a thermostatic water bath. The same experiment was repeated for each temperature. Thermodynamic parameters, enthalpy ΔH° (Kj.mol^{-1}), entropy ΔS° (j. K-1.mol^{-1}) and free energy ΔG° (KJ/mol^{-1}), were determined using the equations:

$$\ln(K_c) = -\frac{\Delta H^{\circ}}{RT} + \frac{\Delta S^{\circ}}{R} \quad (3)$$

$$\Delta G^{\circ} = -RT\ln(K_c) \quad (4)$$

$$\Delta G^{\circ} = \Delta H^{\circ} - T\Delta S^{\circ} \quad (5)$$

where K_C is the equilibrium constant: $K_d = \frac{q_e}{Ce}$.

The observed negative Gibbs free energy values across all examined temperatures signify the feasibility and thermodynamic spontaneity of the biosorption process. (Tong et al., 2011).

The discerned negative enthalpy (ΔH°) conveys the exothermic character of the adsorption interaction, similar results of thermodynamic study were reported (El Atouani et al., 2019) (Table 4).

Table 3
Comparison of maximum adsorption capacities of different seaweed for MB biosorption.

Adsorbent	Q_{max} (mg/g)	Temperature (°C)	References
Cystoseira barbatula	38.61	35	(Caparkaya and Cavas, 2008)
Cystoseira barbata	29.56	25	This study
Cystoseira barbata	12.78	25	(Ozudogru et al., 2017)
Zeolite	12.70	25	(Woolard et al., 2002)
Raw *Posidonia oceanica*	5.56	30	(Ncibi et al., 2007)
C. racemosa var. *cylindracea*	5.23	18	(Cengiz and Cavas, 2008)

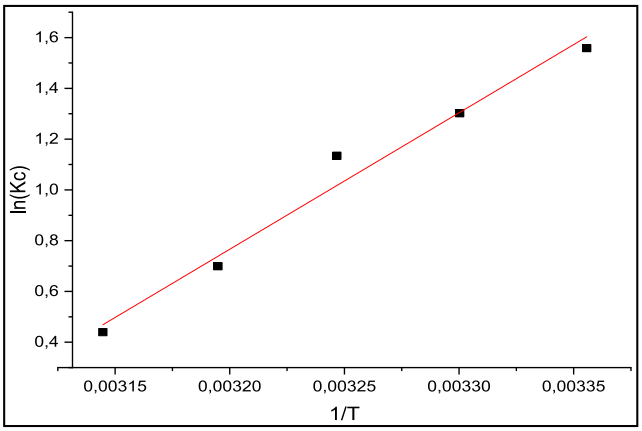

Fig. 13. Right of Van't Hoff equation for MB biosorption.

Table 4
Thermodynamic parameters for MB adsorption on seaweed.

Temperature (K)	ΔH°_{ads} (Kj.mol^{-1})	ΔS°_{ads} (j.K^{-1}.mol^{-1})	ΔG°_{ads} (Kj.mol^{-1})	R^2
298	−44.68	0.15	−89.38	0.97
303			−90.13	
308			−90.88	
313			−91.63	
318			−92.38	

3.4. Mechanism proposal of MB by C.barbata:

Fig. 14 presents FTIR spectroscopy of C. *barbata* before and after biosorption of MB. The proposed adsorption mechanism is illustrated in Fig. 14 (See Fig. 15).

Detection of the main functional groups by FTIR analysis is important in order to investigate the mechanism of MB adsorption by C.*barbata*. On the surface of seaweed biomass, the principle groups detected are hydroxyls, carbonyls and amides. Fig. 13 shows C.*barbata* spectra before and after removal of MB. And exhibits different chemical groups present on seaweed surface that take part in MB adsorption. The bond before MB adsorption at 3404 cm^{-1} moved to 3373 cm^{-1}, confirming the contribution of hydroxyls to the adsorption process. The interaction between hydrogen of hydroxyl groups on the *C.barbata* with positive charge of MB cause an increase of the bond intensity (Kali et al., 2022; Jabri et al., 2023; Amar et al., 2023). Concerning carbonyls, amines and SO_3^{2-} groups, a minor change was detected. The mechanism was mainly governed by the electrostatic interactions according to the study of pH effect (Kali et al., 2022; Loulidi et al., 2020; Loulidi et al., 2020).

4. Conclusion

This work intended to value the effectiveness of marine algae C. *barbata* in methylene blue dye removal from wastewater. From the results obtained, contact time, pH and adsorbent dosage had a major impact on the methylene blue adsorption. The point of zero charge pH_{pzc} value is equal to 8.6 ± 0.1. The equilibrium was reached in 55 min. the value of the maximum adsorption capacity (qm) found was 29.56 mg. g^{-1} at 25 °C. The applicability of Langmuir isotherm model inferred that the adsorption of MB onto the biomass is assumed as a monolayer adsorption. The sorption technique complied successfully with the pseudo-second order kinetic model, which describes better how the sorption process took part on the adsorbent surface. The experimented results showed that C.*barbata* can be considered as an alternative source for MB removal from polluted waters.

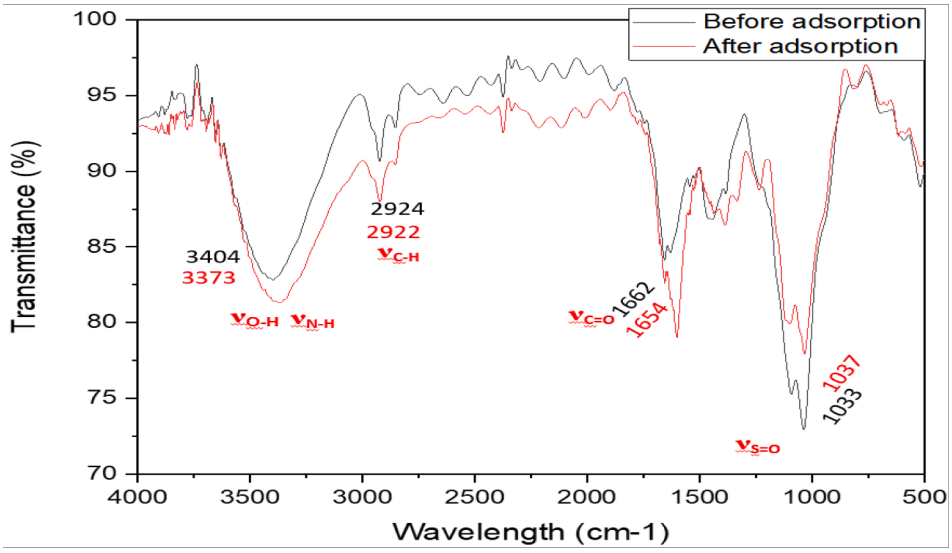

Fig. 14. Principle functional groups by FTIR spectroscopy of C. *barbata* before and after biosorption of MB.

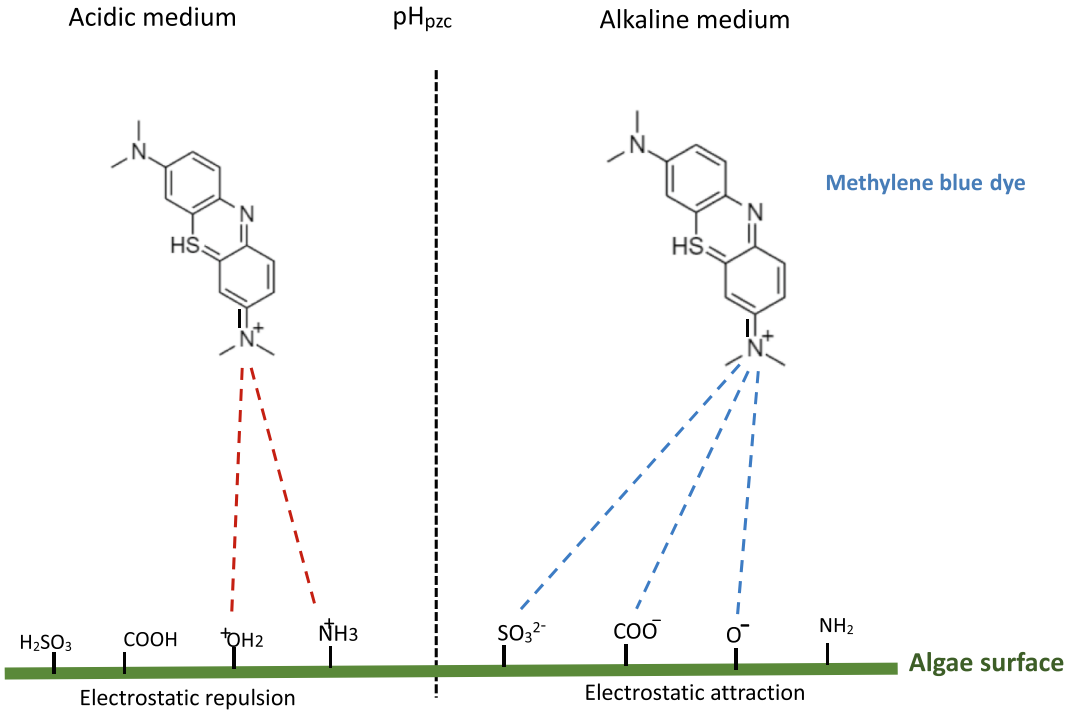

Fig. 15. Biosorption mechanism.

Declaration of competing interest

The authors declare that they have no known competing financial interests or personal relationships that could have appeared to influence the work reported in this paper.

References

Abbood, N.S., Ali, N.S., Khader, E.H., Majdi, H.S., Albayati, T.M., Saady, N.M.C., 2023. Photocatalytic degradation of cefotaxime pharmaceutical compounds onto a modified nanocatalyst. Res. Chem. Intermed. 49 (1), 43–56. https://doi.org/10.1007/s11164-022-04879-3.

Ainane, T., et al., 2014. Removal of hexavalent chromium from aqueous solution by raw and chemically modified seaweed Bifurcaria bifurcata. J. Mater. Environ. Sci. 5 (4), 975–982.

Ali, N.S., et al., 2022. Heliyon Modi fi cation of SBA-15 mesoporous silica as an active heterogeneous catalyst for the hydroisomerization and hydrocracking of n-heptane. Heliyon 8 (May), e09737. https://doi.org/10.1016/j.heliyon.2022.e09737.

Ali, N.S., Kalash, K.R., Ahmed, A.N., Albayati, T.M., 2022. Performance of a solar photocatalysis reactor as pretreatment for wastewater via UV, UV/TiO_2, and UV/H_2O_2 to control membrane fouling. Sci. Rep. 12 (1), 1–10. https://doi.org/10.1038/s41598-022-20984-0.

Ali, N.S., Harharah, H.N., Salih, I.K., Cata Saady, N.M., Zendehboudi, S., Albayati, T.M., 2023. Applying MCM-48 mesoporous material, equilibrium, isotherm, and mechanism for the effective adsorption of 4-nitroaniline from wastewater. Sci. Rep. 13 (1), 1–14. https://doi.org/10.1038/s41598-023-37090-4.

Al-Khodor, Y.A.A., Albayati, T.M., 2023. Real heavy crude oil desulfurization onto nanoporous activated carbon implementing batch adsorption process: equilibrium, kinetics, and thermodynamic studies. Chem. Africa 6 (2), 747–756. https://doi.org/10.1007/s42250-022-00482-6.

Amar, A., et al., 2023. Unveiling the potency of Silica-Alumina-rich clay in phenol remediation and its repurposing prospects. Inorg. Chem. Commun. 154, 110983 https://doi.org/10.1016/j.inoche.2023.110983.

Amar, A., Loulidi, I., Kali, A., Boukhlifi, F., Hadey, C., Jabri, M., 2021. Physicochemical characterization of regional clay: application to phenol adsorption. Appl. Environ. Soil Sci. 2021 https://doi.org/10.1155/2021/8826063.

Belattmania, Z., et al., 2015. Bioremoval of hexavalent chromium from aqueous solutions by the brown seaweed Dictyopteris polypodioides. Res. J. Environ. Toxicol. 9 (5), 218–230. https://doi.org/10.3923/rjet.2015.218.230.

Belattmania, Z., Tahiria, S., Bentiss, F., Sahibed-Dine, A., Jama, C., Zrid, R., Reani, A., Sabour, B., 2017. The residue of alginate extraction from Sargassum muticum (brown seaweed) as a low-cost adsorbent for hexavalent chromium removal from aqueous solutions, Vol. 75, p. 20760. https://doi.org/10.5004/dwt.2017.20760.

Boukhlifi, F., Allali, M., Bencheikh, A., 2001. Étude De La Pollution Métallique Des Eaux Usées D'Une Industrie Chimique Et Essai De Traitement Par La Chitine Brute. Mar. Life 11 (1–2), 49–56.

Boukhlifi, F., Bencheikh, A., 2000. Characterization of natural biosorbents used for the depollution of waste water. Ann. Chim. Sci. Des Materiaux 25 (2), 153–160. https://doi.org/10.1016/s0151-9107(00)88722-x.

Caparkaya, D., Cavas, L., 2008. Biosorption of methylene blue by a brown alga Cystoseira barbatula Kützing. Acta Chim. Slov. 55 (3), 547–553.

Cengiz, S., Cavas, L., 2008. Removal of methylene blue by invasive marine seaweed: Caulerpa racemosa var. cylindracea. Bioresour. Technol. 99 (7), 2357–2363. https://doi.org/10.1016/j.biortech.2007.05.011.

Chcn, G., Pan, J., Han, B., Yan, H., 1999. Adsorption of methylene blue on montmorillonite. J. Dispers. Sci. Technol. 20 (4), 1179–1187. https://doi.org/10.1080/01932699908943843.

Chu, K.H., Hashim, M.A., 2007. Copper biosorption on immobilized seaweed biomass: column breakthrough characteristics. J. Environ. Sci. 19, 928–932.

Cragan, J.D., 1999. Teratogen update: methylene blue. Teratology 60 (1), 42–48. https://doi.org/10.1002/(SICI)1096-9926(199907)60:1<42::AID-TERA12>3.0.CO;2-Z.

El Atouani, S., et al., 2019. Brown seaweed Sargassum muticum as low-cost biosorbent of methylene blue. Int. J. Environ. Res. 13 (1), 131–142. https://doi.org/10.1007/s41742-018-0161-4.

Essekri, A., et al., 2020. Enhanced adsorptive removal of crystal violet dye from aqueous media using citric acid modified red- seaweed : experimental study combined with RSM process optimization. J. Dispers. Sci. Technol. 1–14. https://doi.org/10.1080/01932691.2020.1857263.

Gupta, V.K., Ali Suhas, and D. Mohan, I., 2003. Equilibrium uptake and sorption dynamics for the removal of a basic dye (basic red) using low-cost adsorbents. J. Colloid Interface Sci. 265 (2), 257–264. https://doi.org/10.1016/S0021-9797(03)00467-3.

Heo, J., Yoon, Y., Lee, G., Kim, Y., Han, J., Park, C.M., 2019. Enhanced adsorption of bisphenol A and sulfamethoxazole by a novel magnetic $CuZnFe_2O_4$–biochar composite. Bioresour. Technol. 281 (December 2018), 179–187. https://doi.org/10.1016/j.biortech.2019.02.091.

Jabbar, N.M., Alardhi, S.M., Mohammed, A.K., Salih, I.K., Albayati, T.M., 2022. Challenges in the implementation of bioremediation processes in petroleum-contaminated soils: a review. Environ. Nanotechnology, Monit. Manage. 18 (April), 100694 https://doi.org/10.1016/j.enmm.2022.100694.

Jabri, M., et al., 2023. Valorization of lignocellulosic wastes material for efficient adsorption of a cationic azo dye and sludge recycling as a reinforcement of thermoplastic composite. Fluids 8 (2), pp. https://doi.org/10.3390/fluids8020037.

Jayganesh, D., Tamilarasan, R., Kumar, M., Murugavelu, M., Sivakumar, V., 2017. Equilibrium and modelling studies for the removal of crystal violet dye from aqueous solution using eco-friendly activated carbon prepared from Sargassm Wightii seaweeds. J. Mater. Environ. Sci. 8 (4), 1508–1517.

Kali, A., et al., 2022. Efficient adsorption removal of an anionic azo dye by lignocellulosic waste material and sludge recycling into combustible briquettes. Colloids Interfaces 6 (2), pp. https://doi.org/10.3390/colloids6020022.

Kali, A., et al., 2022. Study of the adsorption properties of an almond shell in the elimination of methylene blue in an aquatic. Moroccan J. Chem. 10 (3), 509–522. https://doi.org/10.48317/IMIST.PRSM/morjchem-v10i3.33140.

Kali, A., et al., 2022. Characterization and adsorption capacity of four low-cost adsorbents based on coconut, almond, walnut, and peanut shells for copper removal. Biomass Convers. Biorefinery. https://doi.org/10.1007/s13399-022-02564-4.

Katiyar, R., Kumar, A., Nguyen, T., Rani, R., Chen, C., Dong, C., 2021. Bioresource technology adsorption of copper (II) in aqueous solution using biochars derived from Ascophyllum nodosum seaweed. Bioresour. Technol. 328 (February), 124829 https://doi.org/10.1016/j.biortech.2021.124829.

Khadim, A.T., Albayati, T.M., Cata Saady, N.M., 2022. Removal of sulfur compounds from real diesel fuel employing the encapsulated mesoporous material adsorbent Co/MCM-41 in a fixed-bed column. Microporous Mesoporous Mater. 341 (June), 112020 https://doi.org/10.1016/j.micromeso.2022.112020.

Khatri, J., Nidheesh, P.V., Anantha Singh, T.S., Suresh Kumar, M., 2018. Advanced oxidation processes based on zero-valent aluminium for treating textile wastewater. Chem. Eng. J. 348 (April), 67–73. https://doi.org/10.1016/j.cej.2018.04.074.

Kumar, M., Elangovan, G., Tamilarasan, R., Vijayakumar, G., Mukeshkumar, P.C., Sendhilnathan, S., 2015. Biosorption of aniline blue from aqueous solution using a novel biosorbent Zizyphus oenoplia seeds: Modeling studies. Polish J. Chem. Technol. 17 (3), 70–77. https://doi.org/10.1515/pjct-2015-0052.

Lesmana, S.O., Febriana, N., Soetaredjo, F.E., Sunarso, J., Ismadji, S., 2009. Studies on potential applications of biomass for the separation of heavy metals from water and wastewater. Biochem. Eng. J. 44 (1), 19–41. https://doi.org/10.1016/j.bej.2008.12.009.

Loulidi, I., et al., 2019. Adsorptive removal of chromium (VI) using walnut. Res. J. Chem. Environ. 23 (12), 25–32.

Loulidi, I., et al., 2020. Kinetic, isotherm and mechanism investigations of the removal of basic violet 3 from water by raw spent coffee grounds. Phys. Chem. Res. 8 (3), 569–584. https://doi.org/10.22036/pcr.2020.225170.1751.

Loulidi, I., et al., 2020. Adsorption of crystal violet onto an agricultural waste residue: kinetics, isotherm, thermodynamics, and mechanism of adsorption. Sci. World J. 2020 https://doi.org/10.1155/2020/5873521.

Maaloul, N., Oulego, P., Rendueles, M., Ghorbal, A., Díaz, M., 2017. Novel biosorbents from almond shells: characterization and adsorption properties modeling for Cu(II) ions from aqueous solutions. J. Environ. Chem. Eng. 5 (3), 2944–2954. https://doi.org/10.1016/j.jece.2017.05.037.

Naciri, Y., et al., 2018. Journal of Environmental Chemical Engineering Facile synthesis, characterization and photocatalytic performance of $Zn_3(PO_4)_2$ platelets toward photodegradation of Rhodamine B dye. J. Environ. Chem. Eng. 6 (2), 1840–1847. https://doi.org/10.1016/j.jece.2018.02.009.

Nassar, M.M., Magdy, Y.H., 1997. Removal of different basic dyes from aqueous solutions by adsorption on palm-fruit bunch particles. Chem. Eng. J. 66 (3), 223–226. https://doi.org/10.1016/S1385-8947(96)03193-2.

Ncibi, M.C., Mahjoub, B., Seffen, M., 2007. Kinetic and equilibrium studies of methylene blue biosorption by Posidonia oceanica (L.) fibres. J. Hazard. Mater. 139 (2), 280–285. https://doi.org/10.1016/j.jhazmat.2006.06.029.

Ozudogru, Y., Merdivan, M., Goksan, T., 2017. Removal of methylene blue from aqueous solutions by brown alga cystoseira barbata. Desalin. Water Treat. 62 (October), 267–272. https://doi.org/10.5004/dwt.2017.20137.

Saffaj, N., et al., 2004. Filtration of solution containing heavy metals and dyes by means of ultrafiltration membranes deposited on support made of moroccan clay. Desalination 168, 301–306.

Sen, T.K., Afroze, S., Ang, H.M., 2011. Equilibrium, kinetics and mechanism of removal of methylene blue from aqueous solution by adsorption onto pine cone biomass of Pinus radiata. Water. Air. Soil Pollut. 218 (1–4), 499–515. https://doi.org/10.1007/s11270-010-0663-y.

Sharma, G., Khosla, A., Kumar, A., Kaushal, N., Sharma, S., 2022. A comprehensive review on the removal of noxious pollutants using carrageenan based advanced adsorbents. Chemosphere 289 (August 2021), 133100. https://doi.org/10.1016/j.chemosphere.2021.133100.

Tong, X., Li, J., Yuan, J., Xu, R., 2011. Adsorption of Cu (II) by biochars generated from three crop straws. Chem. Eng. J. 172 (2–3), 828–834. https://doi.org/10.1016/j.cej.2011.06.069.

Usman, M., et al., 2018. Magnetite and green rust: synthesis properties, and environmental applications of mixed-valent iron minerals. Chem. Rev. https://doi.org/10.1021/acs.chemrev.7b00224.

Woolard, C.D., Strong, J., Erasmus, C.R., 2002. Evaluation of the use of modified coal ash as a potential sorbent for organic waste streams. Appl. Geochem. 17 (8), 1159–1164. https://doi.org/10.1016/S0883-2927(02)00057-4.

Yemendzhiev, H., Koleva, R., Zerrouq, F., Nenov, V., 2021. Utilization of olive mill waste in microbial electrolysis cell. Moroccan J. Chem. 9 (1), 001–006. https://doi.org/10.48317/IMIST.PRSM/morjchem-v9i1.20653.

Zhang, J., Ping, Q., Niu, M., Shi, H., Li, N., 2013. Kinetics and equilibrium studies from the methylene blue adsorption on diatomite treated with sodium hydroxide. Appl. Clay Sci. 83–84, 12–16. https://doi.org/10.1016/j.clay.2013.08.008.